

Controlling the correlations in frequency upconversion in PPLN and PPKTP waveguides

Benjamin Brecht^{*1}, Andreas Eckstein^{1,2}, and Christine Silberhorn^{1,2}

¹ University of Paderborn, Integrated Quantum Optics, Warburger Straße 100, 33098 Paderborn, Germany

² Max Planck Institute for the Science of Light, Günther-Scharowsky-Straße 1 / Bau 26, 91058 Erlangen, Germany

Received 27 August 2010, accepted 30 September 2010

Published online 21 February 2011

Keywords frequency conversion, correlation, single photon, quantum optics

* Corresponding author: e-mail benjamin.brecht@uni-paderborn.de, Phone: +49-5152-605880

Frequency upconversion can be utilized as flexible broadband mode selector for engineered phase matching properties. We give a detailed spectral analysis of frequency upconversion in two different nonlinear waveguides, namely LiNbO_3 and KTiOPO_4 .

We investigate the spectral correlations between input and output photon and derive conditions for their absence. By applying our analysis to the special scenario of upconverting a 1550nm input photon, we find that for this scenario LiNbO_3 is better suited than KTiOPO_4 .

© 2011 WILEY-VCH Verlag GmbH & Co. KGaA, Weinheim

1 Introduction In the context of frequency conversion of single photons it has been shown that it is possible to overcome the limitations of near-infrared (NIR) single photon detectors by upconverting the light to the visible and employing standard Silicon avalanche photo diodes (APDs). By up-converting coherent pulses, which were attenuated to the single photon level, overall efficiencies superior to the detection efficiencies of common NIR APDs have been demonstrated [1–3]. Moreover the successful upconversion of single photons from a real single photon source (a semiconductor quantum dot) has recently been accomplished [4]. In the course of these experiments it has been verified that conversion processes are coherent [5,6] and thus suitable for use in quantum networks. This feature is essential for quantum repeater schemes which necessitate the transduction between visible wavelengths, at which quantum memories typically operate, and telecommunication wavelengths for low-loss transmission over long distances. However, a detailed spectral analysis of the upconversion process is still missing.

Recently a new way of interpreting frequency conversion has been introduced by Raymer et al. [7], who clarified that – for a special case – frequency upconversion is similar to a broadband beamsplitter allowing a Hong-Ou-Mandel-

like interference of photons of different color. In [8] we extended this formalism and illustrated that frequency upconversion can be treated as a broadband mode selector for spectral modes. This will be beneficial in different contexts: By employing our approach not only the output of any photon pair source can be “purified” to generate heralded single photon pulses, but also a new degree of freedom for information coding is in reach as different broadband modes can be read out successively. Careful engineering of the upconversion process is essential to achieve a mapping of input to output wavelengths, which exhibits no spectral correlations, a prerequisite for optimum mode selection. In this paper we present a detailed analysis of the spectral structure of the upconversion in periodically poled LiNbO_3 and KTiOPO_4 waveguides.

2 Theory We consider a sum frequency generation process which is pumped by a bright, pulsed light field (p). A single input photon (in) gets annihilated and an output photon (out) is created. The pump field is not depleted during this process and hence treated classically. We write the

© 2011 WILEY-VCH Verlag GmbH & Co. KGaA, Weinheim

interaction Hamiltonian as

$$\hat{H} = \theta \int d\omega_{in} d\omega_{out} G(\omega_{in}, \omega_{out}) \hat{a}_{in}(\omega_{in}) \hat{c}_{out}^\dagger(\omega_{out}) + \text{h.c.}, \quad (1)$$

where θ describes a pump power dependent coupling constant. The transfer function $G(\omega_{in}, \omega_{out})$ maps the input frequencies ω_{in} to the output frequencies ω_{out} . We have shown in [8] that one can rewrite the transfer function in terms of a Schmidt decomposition to reveal the broadband mode structure of the upconversion process:

$$G(\omega_{in}, \omega_{out}) = \sum_k \lambda_k g_k^{(in)}(\omega_{in}) g_k^{(out)}(\omega_{out}). \quad (2)$$

Moreover, we have established that in order to build an optimal broadband mode selector it is essential that the transfer function exhibits no spectral correlations between input and output frequencies. In terms of broadband modes this can be described by the condition that $G(\omega_{in}, \omega_{out})$ is separable that is

$$G(\omega_{in}, \omega_{out}) = \lambda g^{(in)}(\omega_{in}) g^{(out)}(\omega_{out}). \quad (3)$$

For analyzing this condition with respect to the nonlinear crystal parameters we separate $G(\omega_{in}, \omega_{out})$ into the pump contribution and the phasematching contribution and write

$$G(\omega_{in}, \omega_{out}) = \alpha(\omega_{in}, \omega_{out}) \cdot \phi(\omega_{in}, \omega_{out}), \quad (4)$$

with

$$\alpha(\omega_{in}, \omega_{out}) = \exp\left(-\frac{(\tilde{\omega}_p - \omega_p)^2}{\sigma^2}\right) \quad (5)$$

being the so-called pump envelope function (centered at $\tilde{\omega}_p$ with width σ) which reflects the energy conservation. The function

$$\begin{aligned} \phi(\omega_{in}, \omega_{out}) &= \text{sinc}\left(\frac{L\Delta k(\omega_{in}, \omega_{out})}{2}\right) e^{i\frac{L\Delta k}{2}} \\ &\approx \exp\left[-\gamma\left(\frac{L\Delta k}{2}\right)^2\right] e^{i\frac{L\Delta k}{2}} \end{aligned} \quad (6)$$

describes the phasematching of the process, which is governed by the length of the nonlinear crystal L and the phasemismatch Δk between pump, input and output. It can be approximated by an exponential function with $\gamma \approx 0.193$. When plotted in the $(\omega_{in}, \omega_{out})$ plane the pump envelope function always has a $+45^\circ$ slope as $\omega_p = \omega_{out} - \omega_{in}$. Then again, the slope of the phasematching function is not fixed but depends on the group velocity mismatch between pump, input and output, hence does the amount of spectral correlations in $G(\omega_{in}, \omega_{out})$. This has been considered in great detail for parametric downconversion in [9]. Here we shortly revise the analogous theory for

frequency upconversion in the special case of asymmetric group velocity matching, that is one of the photons – namely the input – travels with the same group velocity as the pump pulse. We chose this restriction for two reasons: firstly, we have shown in [8] that only this configuration allows for an ideal broadband mode selector. The second argument is simply practical: When pump pulse and input photon travel with the same group velocity there is no restriction on the length of the nonlinear crystal as there is no temporal walkoff between pump and input. Thus long crystals can be utilized ensuring high conversion efficiencies at low pump powers and reducing the risk of damaging the crystals. We introduce detunings from the perfect upconversion frequencies as $\nu_j = \tilde{\omega}_j - \omega_j$ with $j = (p, in, out)$. With this we rewrite the pump envelope function as

$$\tilde{\alpha}(\nu_{in}, \nu_{out}) = \exp\left(-\frac{(\nu_{out} - \nu_{in})^2}{\sigma^2}\right). \quad (7)$$

Expanding then the phasemismatch $\Delta k(\omega_{in}, \omega_{out})$ around $\tilde{\omega}_j$ up to second order in frequency we obtain

$$\begin{aligned} L\tilde{\Delta k}(\nu_{in}, \nu_{out}) &= L\Delta k^{(0)} + \tau_{in}\nu_{in} - \tau_{out}\nu_{out} + \\ &+ \beta_{in}^{(+)}\nu_{in}^2 + \beta_{out}^{(-)}\nu_{out}^2 - \\ &- \beta_p\nu_{in}\nu_{out} + \mathcal{O}(\nu^3), \end{aligned} \quad (8)$$

with

$$\begin{aligned} \Delta k^{(0)} &= k_p(\tilde{\omega}_p) + k_{in}(\tilde{\omega}_{in}) - k_{out}(\tilde{\omega}_{out}) - \frac{2\pi}{\Lambda}, \\ \tau_j &= L(k_j^{(1)} - k_p^{(1)}) = L(u_j^{-1} - u_p^{-1}), \\ \beta_j^{(\pm)} &= \frac{L}{2}(k_p^{(2)} \pm k_j^{(2)}), \quad \beta_p = Lk_p^{(2)}. \end{aligned} \quad (9)$$

Here Λ is the optional poling period of the nonlinear crystal and $\Delta k^{(0)}$ must equal zero in order to ensure phase-matching. The index $j = (in, out)$ and $k^{(i)}$ denotes the i th derivative of the wavevector with respect to frequency evaluated at the respective central frequency. The parameters u_j and u_p are the group velocities of input, output and pump inside the crystal. Putting the results from Eq. (7) and (8) into Eq. (4) we find two conditions for $\tilde{G}(\nu_{in}, \nu_{out})$ to develop no spectral correlations similar to those in [9]:

$$\frac{4}{\sigma^2} + \gamma\tau_{in}\tau_{out} = 0, \quad (10)$$

$$2\beta_c + \frac{\beta_p}{2} = 0, \quad (11)$$

where β_c is a parameter describing the chirp of the pump pulse prior to the nonlinear crystal. We will concentrate our analysis on the fulfillment of the first equation as the second condition can be satisfied for in principal any crystal by adjusting the pump chirp. To consider the case where the pump pulse and the input photon have the same group velocities and thus $\tau_{in} = 0$ we express Eq. (10) as:

$$\frac{4}{\sigma^2\tau_{out}} + \gamma\tau_{in} = \frac{4}{\sigma^2\tau_{out}} \stackrel{!}{=} 0. \quad (12)$$

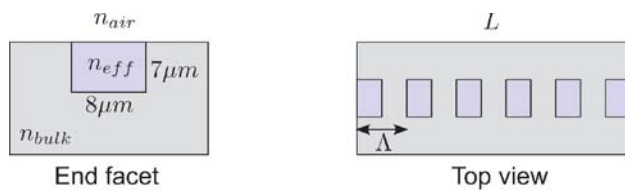


Figure 1 Schematic of the modeled waveguides. The effective refractive index inside the waveguide n_{eff} has been calculated using a dielectric waveguide model.

Note that for long crystals $\tau_{out} \gg \sigma^{-1}$ and therefore the condition for $G(\omega_{in}, \omega_{out})$ to be uncorrelated is fulfilled. In the following sections we will analyze the behavior of the group velocities of the different light fields in two different kinds of nonlinear waveguides.

3 Simulation and results The group velocity of a light field is given by

$$u^{-1} = \frac{1}{c} \left(n(\omega) + \omega \frac{\partial n(\omega)}{\partial \omega} \right), \quad (13)$$

where $n(\omega)$ is the frequency dependent refractive index of the material under consideration. This necessitates the modeling of the refractive index of the nonlinear waveguides. To ensure a good comparability between the PPLN and the PPKTP waveguides we use a dielectric waveguide model for both materials. We assume a constant refractive index difference between the waveguide and the surrounding material of $\Delta n = 0.01$ and model waveguides with a realistic size of $8 \times 7 \mu\text{m}^2$ (compare Fig. 1) and a length of 50mm. The bulk Sellmeier equations are taken from [10] and [11] for LiNbO₃ and from [12] for KTP, respectively. We concentrate on two detailed examples with the input being at 1550 nm. This choice is motivated by the fact that photons, which get upconverted, have been typically transmitted via fibre networks beforehand. Moreover, as we already mentioned the possibility to "purify" the output of a photon pair source, this scenario allows for the realization of a heralded source of single photon pulses at telecom wavelengths. Note however that the analysis is applicable to any desired combination of input, output and pump wavelengths.

3.1 PPLN In Fig. 2 we plot the group refractive indices of the PPLN waveguide for ordinary and extraordinary polarization at a temperature of $T = 185^\circ\text{C}$. If pump and input are oriented along the same direction, there is only one way to generate an uncorrelated $G(\omega_{in}, \omega_{out})$: the pump must have the exact same wavelength as the input. In this case however, it is not possible to separate the converted input photon from the inevitable second harmonic of the pump. Thus a type II process is needed such that the pump and input are oriented along different directions. From Fig. 2 it is obvious that, if the input is on the extraordinary axis, no pump wavelength can be found such that a pump oriented along the ordinary axis has the same

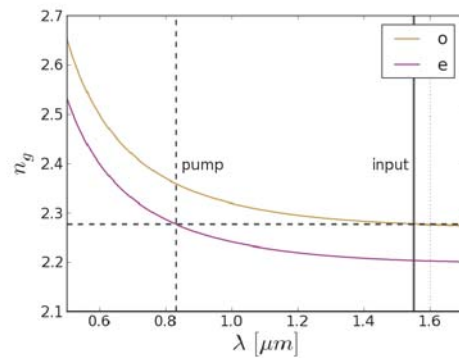


Figure 2 Group refractive indices for PPLN waveguide. The input wavelength of 1550 nm and the resulting pump wavelength are marked.

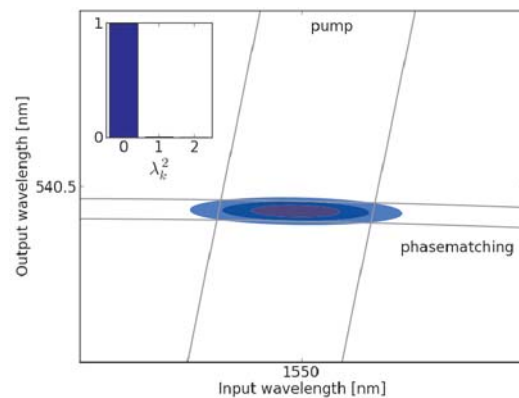


Figure 3 Transfer function $G(\omega_{in}, \omega_{out})$ for the conversion in PPLN. The inset shows the λ_k^2 (compare Eq. (2)). Only one coefficient differs notably from 0 thus $G(\omega_{in}, \omega_{out})$ is uncorrelated.

group refractive index as the input. Therefore the only scenario, in which a broadband mode selector can be realized is the one depicted in Fig. 2. The input is launched on the ordinary axis and the pump on the extraordinary axis, respectively. One then finds that a pump with a center wavelength of 830nm satisfies the requirement of having the same group refractive index as the input, and thus it travels at the same speed through the nonlinear crystal. The output is oriented along the ordinary axis in this case. In Fig. 3 we plot the transfer function $G(\omega_{in}, \omega_{out})$. The inset shows the square of the coefficients λ_k in the Schmidt decomposition (see Eq. (2)), which give the probability that the input is in mode $g_k^{(in)}(\omega_{in})$ and the output in mode $g_k^{(out)}(\omega_{out})$, respectively. As only one coefficient differs from zero, $G(\omega_{in}, \omega_{out})$ is in fact uncorrelated and this up-conversion process can be described as broadband mode selector. The temperature of 185°C is beneficial as the photorefractive damage in PPLN is lower here than at room

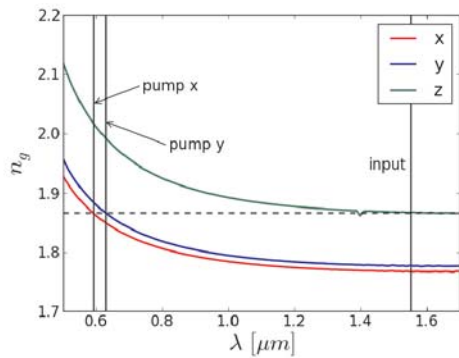


Figure 4 Group refractive indices for KTP waveguide. The input wavelength of 1550 nm and the resulting pump wavelengths are marked.

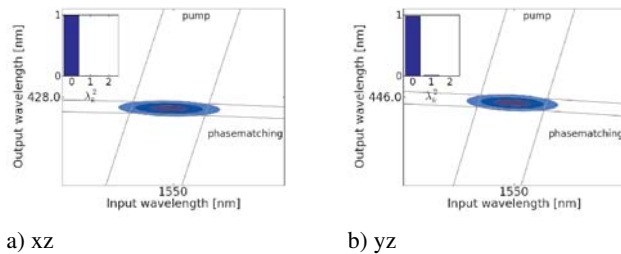


Figure 5 Mapping functions $G(\omega_{in}, \omega_{out})$ of the two possible conversion processes in PPKTP. The insets show the λ_k^2 of the Schmidt decompositions (see Eq. (2)). Both mapping functions are uncorrelated.

temperature. Moreover the resulting pump wavelength of 830nm is inside the Ti:Sa spectrum and a huge range of different pump pulse lengths and shapes can be generated here. This is a prerequisite for flexible broadband mode selection as we pointed out in [8]. The output wavelength of around 540nm is in the visible and can thus be detected with high efficiency. The only drawback of this scenario is the poling period of the PPLN crystal which turns out to be $\Lambda \approx 4\mu\text{m}$ which is technically quite challenging. Note that higher temperatures lead to the pump wavelength moving towards higher wavelengths. However, for a pump wavelength of around 1064nm, crystal temperatures of around 800°C would be needed. This is technically almost impossible to accomplish as the whole crystal would have to be heated absolutely homogenously. We therefore did not consider those cases in detail.

3.2 PPKTP In Fig. 4 we plot the group refractive indices of the PPKTP waveguide for different polarizations of the light fields. The cut of the nonlinear crystal defines which refractive indices correspond to the waveguide axes. The input wavelength of 1550 nm is marked with a black line. As with the PPLN waveguide only type II processes

can fulfill the condition of input and pump pulse having the same group refractive index. The only type II processes which are allowed in KTP are processes involving the z axis. Thus, the case of pump and input being oriented along x and y direction is forbidden. One can see that the input with central frequencies in the range of 1550 nm has to be oriented along z direction in order to find a suitable pump wavelength. Then two different possible solutions can be identified. If the pump is oriented along the y its corresponding wavelength lies around 627 nm. For an orientation of the pump along the x axis its central frequency has to be chosen around 592 nm. The outputs are in both cases oriented along the same axis as the pump and have wavelength of 446 nm or 428 nm, respectively. In Fig. 5 we plot the two transfer functions $G(\omega_{in}, \omega_{out})$ and the corresponding squared Schmidt coefficients λ_k^2 . Both processes (xz→x left and yz→y right) result in uncorrelated transfer functions and can thus serve as broadband mode selectors. Note that changing the temperature does not influence the wavelengths as dramatically as is the case with PPLN and is therefore not treated here in detail. While the poling periods of the PPKTP crystal are roughly 13μm (12μm), which is preferable in terms of waveguide fabrication, the pump wavelengths and the resulting output wavelengths are less favorable due to difficulties in reaching such pump wavelengths and low detector efficiencies in the blue visible wavelength regime. This brings us to the conclusion that – for this special upconversion scenario – PPLN would be more applicable than PPKTP for experimental implementations.

Acknowledgements This work was supported by the EC under the FET-Open grant agreement CORNER, number FP7-ICT-213681.

References

[1] M. A. Albota and F. N. C. Wong, *Opt. Lett.* **29**(13) (2004).
 [2] C. Langrock, E. Diamanti, R. V. Roussev, Y. Yamamoto, M. M. Fejer, and H. Takesue, *Opt. Lett.* **30**(13) (2005).
 [3] A. P. VanDenvender and P. G. Kwiat, *J. Opt. Soc. Am. B* **24**(2) (2007).
 [4] M. T. Rakher, L. Ma, O. Slattery, X. Tang, and K. Srinivasan, arXiv:1004.2686v1 (2010).
 [5] J. Huang and P. Kumar, *Phys. Rev. Lett.* **68**(14) (1992).
 [6] S. Tanzilli, W. Tittel, M. Halder, O. Alibart, P. Baldi, N. Gisin, and H. Zbinden, *Nature* **437**(1) (2005).
 [7] M. G. Raymer, S. J. van Enk, C. J. McKinstrie, and H. J. McGuinness, arXiv:1002.0350v1 (2010).
 [8] A. Eckstein, B. Brecht, and C. Silberhorn, arXiv:1007.3215v1 (2010).
 [9] A. B. U'Ren, C. Silberhorn, K. Banaszek, I. A. Walmsley, R. Erdmann, W. P. Grice, and M. G. Raymer, *Laser Physics* **15**(1) (2005).
 [10] G. J. Edwards and M. Lawrence, *Opt. Quantum Electron.* **16** (1984).
 [11] D. H. Jundt, *Opt. Lett.* **22**(20) (1997).
 [12] K. Kato and E. Takaoka, *Appl. Opt.* **41**(24) (2002).